International Journal of Control, Automation, and Systems 21(10) (2023) 3336-3347
http://dx.doi.org/10.1007/s12555-022-0715-2
ISSN:1598-6446 eISSN:2005-4092
http://www.springer.com/12555

# Nonlinear Predictive Control of Active Four-wheel Steering Vehicles

**Shuyou Yu*, Wenbo Li, Yongfu Li, Hong Chen, Hongqing Chu, Baojun Lin, and Jianhua Yu**

**Abstract:** In order to improve the handling stability of active four-wheel steering vehicles, a nonlinear model predictive controller is presented, which can guarantee that the actual sideslip angle and yaw rate can track the ideal sideslip angle and the ideal yaw rate through control of the front and rear wheel angles. A nonlinear static tyre model connected with a linear dynamic model is adopted to describe the vehicle dynamics. Furthermore, the tyre model is replaced by a map in the optimization problem of nonlinear model predictive control. The introduction of maps can reduce the online computational time by a trade-off between the computational burden of CPU and the storage burden of ROM. Simulation results in CarSim indicate that the proposed controller can follow the outputs of the ideal reference model, reduce the computational burden, and improve the handling stability of the active four-wheel steering vehicles effectively.

**Keywords:** Active four-wheel steering, computation efficiency, handling stability, hash table, model predictive control.

## 1. INTRODUCTION

Enhancing the handling stability of vehicles is a promising way to address road safety. Therefore, chassis control technologies which can improve vehicle stability have received extensive attention [1-3]. Active four-wheel steering (4WS), which is one of the chassis control technologies, is gaining a lot of attention because of its role in improving the handling stability of vehicles [4]. Applications of active rear-wheel steering have been demonstrated [5,6]. Nevertheless, it is a typical single-input single-output system, which has limited effectiveness in improving vehicle handling stability [7-10]. By controlling the front and rear wheel angle effectively, the active four-wheel steering system can improve the vehicle's steering characteristics, and keep the steady-state gains of the lateral acceleration and the yaw rate are small while the vehicle is steering [11-13].

A lot of controllers have been proposed to improving the handling stability of 4WS vehicles based on the assumption that the tyre slip angle is small, i.e., the tyre force has a linear relationship with the tyre slip angle. A sliding mode control is presented for the active four-wheel steering systems, in which a time-varying sliding surface is designed to eliminate steady-state errors and a smooth function is designed to alleviate the chattering effect [14]. An internal mode decoupling scheme is developed to enhance the robustness of 4WS system by rejecting saturation and delay of actuators [15]. Considering parametric uncertainties and disturbances, an adaptive integral terminal sliding mode controller for 4WS vehicles with Ackerman Geometry is presented in [16]. A feedforward and feedback controller, which takes into account disturbances and unmodeled dynamics of systems, is presented to track desired signals of a reference model [17]. A mixed $H_2/H_\infty$ robust control method is proposed for the purpose of ensuring stability, robustness, and performance of systems [18,19]. A control law composed of state and disturbance feedback controls is proposed to compensate the influence of disturbances on 4WS [20]. To enhance handling stability of 4WS vehicles, a triple-step steering controller based on a linear tyre model has been developed

Manuscript received July 28, 2022; revised January 12, 2023; accepted February 22, 2023. Recommended by Associate Editor Alessandro Giuseppi under the direction of Editor-in-Chief Hyo-Sung Ahn. This work is supported by the National Natural Science Foundation of China (No.U1964202), the Foundation of State Key Laboratory of Automotive Simulation and Control, the Foundation of Key Laboratory of Industrial Internet of Things and Networked Control (No.2019FF01), and the Science Foundation of Jilin Province (No.YDZJ202101ZYTS169).

Shuyou Yu is with the State Key Laboratory of Automotive Simulation and Control, Jilin University, Changchun 130025, China, and also with the Department of Control Science and Engineering, Jilin University, Changchun 130025, China (e-mail: shuyou@jlu.edu.cn). Wenbo Li and Baojun Lin are with the Department of Control Science and Engineering, Jilin University, Changchun 130012, China (e-mails: liwb21@mails.jlu.edu.cn, linbj@jlu.edu.cn). Yongfu Li is with the College of Automation, Chongqing University of Posts and Telecommunications, Chongqing 400065, China (e-mail: liyongfu@cqupt.edu.cn). Hong Chen is with the College of Electronics and Information Engineering, Tongji University, Shanghai 200092, China, and also with the Department of Control Science and Engineering, Jilin University, Changchun 130025, China (e-mail: chenh@jlu.edu.cn). Hongqing Chu is with the School of Automotive Studies, Tongji University, Shanghai 200092, China (e-mail: chuhongqing@tongji.edu.cn). Jianhua Yu is with the Dongfeng Commercial Vehicle Technology Center, Wuhan 430058, China (e-mail: yujh@dfcv.com.cn).
* Corresponding author.

 

[21], which can realize self-regulation of time-varying parameters. Furthermore, model predictive control (MPC) strategies, which allow to explicit handle constraints, have been presented for 4WS vehicles [22-25]. A model predictive controller considering constraints of actuators, tyre slip angles, and lateral acceleration is designed for the 4WS vehicle to follow a reference yaw angle, and a reference longitudinal displacement [26]. Considering the inner coupling between the front and rear wheels of vehicles, a double-layer dynamic decoupling controller is proposed to guarantee lateral stability of the 4WS vehicle, in which a lower part-steering control unit is designed to obtain decoupled control signals by model predictive controller [27].

In principle, the tyre lateral characteristic is nonlinear, for example, while the lateral acceleration is large. Considering parameter-varying property of tyre cornering stiffness, a robust adaptive sliding mode controller is designed, in which a Takagi-Sugeno fuzzy model is established to represent the nonlinear characteristics of tyres [28]. A linear quadratic optimal control with the weighted function of tyre cornering stiffness is adopted to achieve satisfying performance when the tyre slip angle is large or the vehicle is driving on a low adhesion road [29]. Considering the nonlinear characteristics of tyres, a nonlinear triple-step controller with a map is designed in [30] to enhance the handling stability of 4WS vehicles. In order to minimize the tracking errors of the lateral displacement and the yaw angle of a 4WS vehicle, a model predictive controller is designed, in which the nonlinear characteristics of tyres is described by Magic Formula [31]. A model predictive controller is to improve the driving performance of four-wheel independent steering vehicles, in which a nonlinear vehicle model is fitted by a neural network, and coincidence degree of wheel steering centers is chosen as a performance index [32]. On one hand, existing kinds of literature mainly design controllers to enhance the handling stability of 4WS based on the linear tyre model, Magic Formula tyre model, or short wavelength intermediate frequency tyre model, etc. On the other hand, unmodeled dynamics of the load variation of tyres and constraints of the actuators, the sideslip angle, and the yaw rate are not taken into account simultaneously.

In this paper, a novel modeling method for active four-wheel steering vehicles is proposed, in which the tyres based on a map are first introduced. Then, an efficient lookup table algorithm is proposed, and a model predictive controller is designed where the nonlinear lateral characteristics of tyres, the constraints of the actuator, the sideslip angle, and the yaw rate are considered. Compared with the traditional tyre models, the lookup table can fully characterize the nonlinearity of the tyre, which converts the computational burden into the storage burden.

The paper is organized as follows: Section 2 sets up the control problems and derives the dynamic model of the 4WS vehicle. Section 3 introduces the steering nonlinear model predictive controller. Section 4 verifies the effectiveness of the proposed controller through simulation. The conclusion is drawn in Section 5.

## 2. PROBLEM SETUP

In general, the purpose of an active four-wheel steering system is to improve vehicle handling stability. In this research, improving the vehicle handling stability will be transformed into the problem of tracking the ideal steering characteristics. Suppose that the sideslip angle and the tyre load can be accurately observed. The 4WS vehicle control system is shown in Fig. 1. The ideal sideslip angle $\beta^*$ and the ideal yaw rate $\gamma^*$ are determined by the reference model based on the reference front wheel angle $\delta_f^*$. The steering angles of the front and rear wheels, i.e., $\delta_f$, $\delta_r$, are determined by model predictive controller in terms of the tyre loads of the front and rear wheel $F_{zi}$, $i = f, r$, and errors between $\beta^*$, $\gamma^*$ and $\beta$, $\gamma$.

### 2.1. Vehicle model without the property of tyres

A two-degree-of-freedom vehicle model is presented in this research, which can reflect the basic steering characteristics of an active four-wheel steering vehicle, as shown in Fig. 2.

In Fig. 2, $\beta$ is the sideslip angle, $\alpha_f$ and $\alpha_r$ are the slip angle of the front and rear tyres respectively, $v$ is the longitudinal speed, $v_y$ is the lateral speed, $F_{yf}$ is the lateral force of the front wheel, $\delta_f$ is the front wheel angle, $F_{yr}$ is the lateral force of the rear wheel, $\delta_r$ is the rear wheel angle, $a$ and $b$ are distances from the center of gravity to the front and rear axle respectively, $m$ is the vehicle mass,

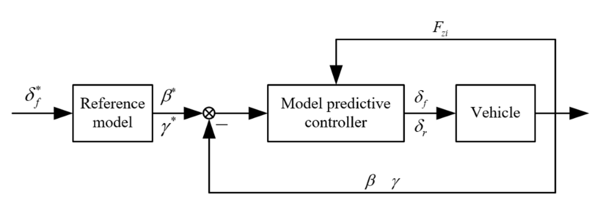


Fig. 1. 4WS vehicle control system.

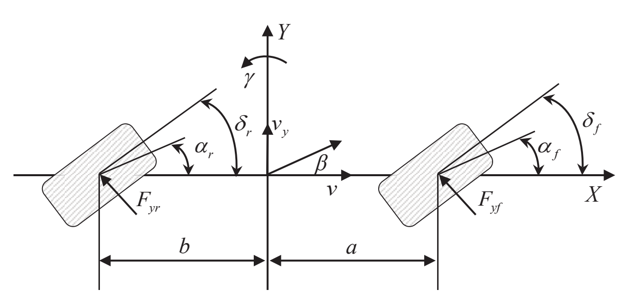


Fig. 2. Two degree-of-freedom vehicle model without the property of tyres.

Table 1. Table of of tyre side characteristics.

| $F_{zi}$ $(N)$ / $\alpha_i$ (deg) | 0 | 2200 | 4125 | 6250 | 8105 | 10525 |
|---|---|---|---|---|---|---|
| 0 | 0 | 0 | 0 | 0 | 0 | 0 |
| 0.5 | 0 | 371.57 | 678.85 | 941.63 | 1081.15 | 1129.98 |
| 1 | 0 | 711.74 | 1286.92 | 1794.96 | 2134.63 | 2259.97 |
| ⋮ | ⋮ | ⋮ | ⋮ | ⋮ | ⋮ | ⋮ |
| 20.5 | 0 | 1645.8 | 3285.59 | 4932.07 | 6586.24 | 8237.64 |

and $\gamma$ is the yaw rate.

The vehicle model without the property of tyres is [19]

$$\begin{aligned} mv\left(\dot{\beta}+\gamma\right) &= F_{yf}+F_{yr}, \\ I_z\dot{\gamma} &= aF_{yf}-bF_{yr}, \end{aligned} \tag{1}$$

where $I_z$ is the yaw moment of inertia.

### 2.2. Tyre model

According to (1), the steering characteristics of 4WS vehicles are determined primarily by lateral forces of tyres. A nonlinear map of $F_{yi}$ with respect to $\alpha_i$ and $F_{zi}$, $i = f, r$, is shown in Fig. 3. The data of side characteristics of tyres in this research are obtained from a CarSim's tyre model $(215/79\ R15)$. Tyre model can be classified into the physical model and the empirical model [33]. On one hand, physical models in general are too complex to be implemented in real-time operations compared to empirical models. On the other hand, empirical models, for example the Magic formula and the Dugoff model, rely on a number of full-scale tests since there are a lot of parameters to fit data accurately [34], which might cause a heavy online computational burden in MPC as well.

A tyre model based on a map is presented here, in which the lateral force is obtained by lookup-table methods, cf. Table 1. The table includes $n_{row}$ rows and $n_{col}$ columns,

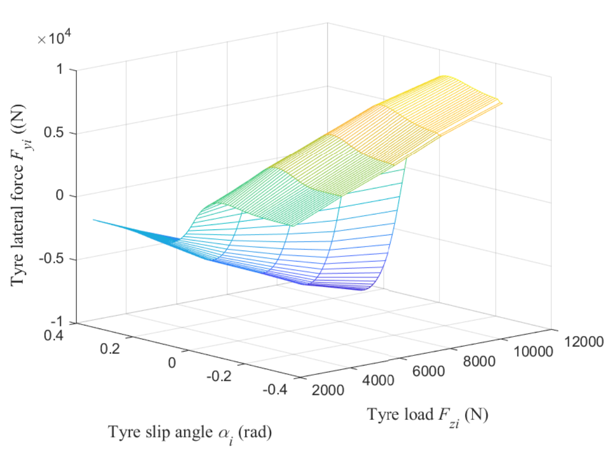


Fig. 3. Curve of tyre side characteristics.

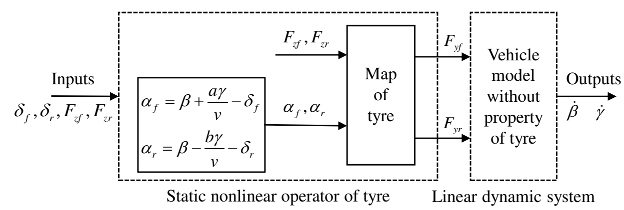


Fig. 4. Two degree-of-freedom vehicle model.

where the first column and the first row store the keywords of the tyre slip angle and the tyre load, respectively.

### 2.3. Vehicle model

A nonlinear vehicle model is established [35], which includes a static nonlinear operator of tyre and a linear dynamic system, as shown in Fig. 4.

The tyre slip angles of the front and rear wheel are [36]

$$\begin{aligned} \alpha_f &= \beta + \frac{a\gamma}{v} - \delta_f, \\ \alpha_r &= \beta - \frac{b\gamma}{v} - \delta_r. \end{aligned} \tag{2}$$

Choosing the state $x = \begin{bmatrix}\beta & \gamma\end{bmatrix}^T$ and the control input $u = \begin{bmatrix}\delta_f & \delta_r\end{bmatrix}^T$, the two degree-of-freedom four-wheel steering vehicle based on the map is described as

$$\begin{cases} F_{yf} = F_{mapf}\left(x, u, F_{zf}\right), \\ F_{yr} = F_{mapr}\left(x, u, F_{zr}\right), \\ \dot{x} = Ax + Bu_F, \end{cases} \tag{3}$$

where $u_F = \begin{bmatrix}F_{yf} & F_{yr}\end{bmatrix}^T$, $F_{mapf}$ and $F_{mapr}$ are the nonlinear map of tyre, i.e., Fig. 3, and

$$A = \begin{bmatrix} 0 & -1 \\ 0 & 0 \end{bmatrix},\ B = \begin{bmatrix} \frac{1}{mv} & \frac{1}{mv} \\ \frac{a}{I_z} & \frac{-b}{I_z} \end{bmatrix}. \tag{4}$$

## 3. THE NONLINEAR STEERING CONTROLLER

### 3.1. Reference model

Here, a reference model is adopted in order to provide the ideal steering characteristics for 4WS vehicles. The steering sensitivity of 4WS vehicles is required to be the same as that of the traditional vehicle, and the sideslip angle is required to be close to zero after adding a rear wheel angle. Then, the reference model is [37,38]

$$\dot{x}_d = A_d x_d + B_d u_d, \tag{5}$$

with

$$A_d = \begin{bmatrix} -\frac{1}{\tau_\beta} & 0 \\ 0 & -\frac{1}{\tau_\gamma} \end{bmatrix},\ B_d = \begin{bmatrix} \frac{k_\beta}{\tau_\beta} \\ \frac{k_\gamma}{\tau_\gamma} \end{bmatrix}, \tag{6}$$

where $x_d = \begin{bmatrix} \beta^* & \gamma^* \end{bmatrix}^T$ is the state of the reference model, i.e., the ideal sideslip angle and the ideal yaw rate, $u_d = \begin{bmatrix} \delta_f^* \end{bmatrix}$ is the input of the reference model, i.e., the reference front wheel angle. The terms of $\tau_\beta$ and $\tau_\gamma$ are the time constants, $k_\beta$ is the steady state gain of the ideal sideslip angle, and the steady state gain of the ideal yaw rate is [39]

$$k_\gamma = \frac{C_f C_r (a+b) v}{C_f C_r (a+b)^2 - mv^2 (aC_f - bC_r)}, \tag{7}$$

where $C_f$ is the front wheel side cornering stiffness, and $C_r$ is the rear wheel side cornering stiffness.

Note that usually $k_\beta$ is small, which can even be set to zero in the ideal situation. The empirical range of $\tau_\beta$ and $\tau_\gamma$ is generally 0.01-0.3, respectively [39].

Considering the limitation of road adhesion conditions, the acceleration constraint of a vehicle is [40]

$$|a_y| \leq \mu g, \tag{8}$$

where $\mu$ is the road adhesion coefficient, and $g$ is the constant of gravitation. Denote a set $S_\gamma$ as

$$S_\gamma := \left\{ S \in R^1 \,\middle|\, |S| \leq \frac{\mu g}{v} \right\}. \tag{9}$$

The yaw rate $\gamma$ satisfies $\gamma \in S_\gamma$, and the ideal yaw rate $\gamma^*$ stays in the same saturation region as well, i.e., $\gamma^* \in S_\gamma$ [41].

**Remark 1:** In general, the goal of chassis control technologies is to design a controller to make the vehicle with the handling stability [42,43]. The conditions of the handling stability are given by the reference model [37,38]. Note that theoretical studies on the handling stability are beyond the scope of this research.

### 3.2. Predictive controller with tyre map

The stability control problem for active four-wheel steering vehicles can be transformed into a trajectory tracking control problem. The state and input constraints are

$$X := \left\{ x = \begin{bmatrix} \beta & \gamma \end{bmatrix}^T \,\middle|\, |\beta| \leq \beta_{max},\ |\gamma| \leq \frac{\mu g}{v} \right\}, \tag{10}$$

$$U := \left\{ u = \begin{bmatrix} \delta_f & \delta_r \end{bmatrix}^T \,\middle|\, |\delta_f| \leq \delta_{fmax},\ |\delta_r| \leq \delta_{rmax} \right\}, \tag{11}$$

where $\beta_{max}$ is an upper limit of the sideslip angle, $\delta_{fmax}$ and $\delta_{rmax}$ are upper limits of the front and rear wheel angle, respectively.

Considering constraints of the actuators, the sideslip angle, and the yaw rate, the optimization problem is formulated as follows:

**Problem 1:**

$$\underset{u(\cdot)}{\text{minimize}}\ J_1(u(\cdot)), \tag{12}$$

subject to

$$\begin{cases} F_{yf}(\tau, x(t)) = F_{mapf}(x(t), u(\tau), F_{zf}(t)), \\ F_{yr}(\tau, x(t)) = F_{mapr}(x(t), u(\tau), F_{zr}(t)), \\ \dot{x}(\tau, x(t)) = Ax(\tau, x(t)) + Bu_F(\tau, x(t)), \\ u(\tau) \in U, \\ x(\tau, x(t)) \in X, \\ x(t, x(t)) = x(t), \\ \tau \in [t, t+T_p], \end{cases} \tag{13}$$

where

$$J_1(u(\cdot)) := \int_t^{t+T_p} \Big( \|x(\tau, x(t)) - x_d(\tau)\|_Q^2 + \|\Delta u(\tau)\|_R^2 \Big) d\tau \tag{14}$$

is the cost function.

In Problem 1, $T_p$ is the prediction horizon, $x(\cdot, x(t))$ represents the predicted state trajectory starting from the initial state $x(t)$ under the control $u(\cdot)$, $Q$ and $R$ are positive definite state and input weighting matrices, respectively. Problem 1 is solved in discrete time, in which the sampling time is $\Delta t$, and $\Delta u(\tau) = u(\tau) - u(\tau - \Delta t)$.

**Remark 2:** Problem 1 usually requires to solve a Hamilton-Jacobi-Bellman (HJB) equation. However, the analytical solution of the HJB equation cannot be obtained directly in general. Therefore, the methods to obtain numerical solution is adopted, for example sequential quadratic programming (SQP), the Newton-type method, heuristic algorithms. Since Problem 1 contains look-up tables, it cannot be directly solved by the gradient-based optimization algorithm, i.e., SQP, Newton-type method. Herein, the heuristic algorithms are adopted, such as the particle swarm optimization algorithm, the ant colony optimization algorithm, and the simulate anneal arithmetic.

### 3.3. Optimization algorithm

In this research, the particle swarm optimization algorithm is used to solve Problem 1. Since particle swarm optimization algorithm can not solve directly constrained optimization problem [44], the cost function $J_1$ is rewritten as

$$J_2(u(\cdot)) := \int_t^{t+T_p} \Big( \|x(\tau, x(t)) - x_d(\tau)\|_Q^2$$

$$+ \left.\|\Delta u(\tau)\|_R^2 + \sigma P_{en}(\tau)\right) d\tau, \tag{15}$$

where $\sigma$ is a positive penalty coefficient, and $P_{en}(t)$ is a penalty function

$$P_{en}(\tau) = \max\{0, C_j(x(\tau, x(t)), u(\tau))\}, \quad j = 1,\ 2,\ 3,\ 4, \tag{16}$$

with

$$\begin{cases} C_1((x(\tau,x(t)),u(\tau))) = |\beta(\tau)| - \beta_{max}, \\ C_2((x(\tau,x(t)),u(\tau))) = |\gamma(\tau)| - \dfrac{\mu g}{v}, \\ C_3((x(\tau,x(t)),u(\tau))) = |\delta_f(\tau)| - \delta_{fmax}, \\ C_4((x(\tau,x(t)),u(\tau))) = |\delta_r(\tau)| - \delta_{rmax}. \end{cases} \tag{17}$$

Thus, the optimization problem can be rewritten as

**Problem 2:**

$$\underset{u(\cdot)}{\text{minimize}}\ J_2(u(\cdot)), \tag{18}$$

subject to

$$\begin{cases} F_{yf}(\tau,x(t)) = F_{mapf}(x(t),u(\tau),F_{zf}(t)), \\ F_{yr}(\tau,x(t)) = F_{mapr}(x(t),u(\tau),F_{zr}(t)), \\ \dot{x}(\tau,x(t)) = Ax(\tau,x(t)) + Bu_F(\tau,x(t)), \\ x(t,x(t)) = x(t), \\ \tau \in [t, t+T_p]. \end{cases} \tag{19}$$

The proposed nonlinear model predictive control law is formally described by Algorithm 1.

### 3.3.1 Hash table

At Step 4 of Algorithm 1, the computational complexity of Problem 2 is mainly caused by the nonlinear tyre model. A lookup-table method is presented to compute the tyre lateral force, which is established by tyre lateral characteristic, i.e., Table 1. Note that the nonlinear optimal problem is transformed into a linear optimization problem, and computation complexity is replaced by the related astorage and search complexities.

---

**Algorithm 1:** 4WS vehicle control system.

---

**Input:** $\beta$, $\gamma$, $\delta_f^*$, $F_{zi}\,(i = f, r)$
**Output:** $\delta_f$, $\delta_r$
**Step 1:** Initialization.
**Step 2:** Get values of $x(t)$ and $F_{zi}(t)$.
**Step 3:** Compute the ideal sideslip angle and yaw rate, i.e., $\beta^*$, $\gamma^*$, by reference model.
**Step 4:** Solve Problem 2 to get $u^*(\cdot)$.
**Step 5:** The first element of the open-loop control sequence acts on the system.
**Step 6:** At the next time instant, set $t = t + \Delta t$, and go to Step 2.

---

Here, the hash table is used to obtain the lateral forces based on the tyre slip angles and the tyre loads. The hash table is made up of two parts: a matrix (the actual table that stores data of tyre side characteristics, i.e., Table 1), and a hash function [45].

Denote $M$ as a matrix consisting of data in Table 1. Denote $M(k,c)$ with $k = 1, 2, \cdots, row$ and $c = 1, 2, \cdots, col$ as the element located in the $k$-th raw and $c$-th column of $M$. Furthermore, define a submatrix of $M$ as

$$M(r:k,c) = [M(r,c), M(r+1,c), \cdots, M(k,c)]^T. \tag{20}$$

For every tyre load $F_{zi}$, there is a positive integer $n_1$ such that

$$M(1,n_1) \le F_{zi} < M(1,n_1+1), \quad 2 \le n_1 < n_{col}, \tag{21}$$

where $n_1$ is calculated by the sequential search method [46].

Then, according to (21), a submatrix $\tilde{M}$ consisting of the tyre lateral forces under the tyre load $F_{zi}$, can be obtained by the linear interpolation [47].

$$\begin{aligned} &\tilde{M}(1:n_{col}-1,1) \\ &= M(2:n_{col},n_1) \\ &\quad + \frac{F_{zi} - M(1,n_1)}{M(1,n_1+1) - M(1,n_1)} \\ &\quad \times (M(2:n_{col},n_1+1) - M(2:n_{col},n_1)). \end{aligned} \tag{22}$$

Denote $[\alpha_0,\ \alpha_n]$ as the interval of the tyre slip angle in Table 1, where $\alpha_0 = 0$, $\alpha_n = 20.5$, and $n = 41$. Divide each interval into equal parts, and encode them as 1, 2, …, $n$. Considering the hash function $ceil(\cdot)$ mapping a real number to an integer, i.e., roundup function, the keyword for any $F_{yf}$ or $F_{yr}$ are $(n_1, n_2)$, where

$$n_2 = ceil\left((|\alpha_i| - \alpha_0)\frac{n}{\alpha_n - \alpha_0}\right). \tag{23}$$

Furthermore, the lateral force $F_{yi}$ can be obtained by following linear interpolation, i.e.,

$$\begin{aligned} F_{yi}(\alpha_i) = -sign(\alpha_i)\Big[&\tilde{M}(n_2,1) \\ &+ \frac{|\alpha_i| - \alpha_{n_2}}{\alpha_{n_2+1} - \alpha_{n_2}}(\tilde{M}(n_2+1,1) - \tilde{M}(n_2,1))\Big]. \end{aligned} \tag{24}$$

The algorithm of tyre model based on the hash table is formulated as Algorithm 2.

## 4. SIMULATION

In this research, CarSim's tyre model $(215/70\ R15)$ is used. A table of tyre shown in Table 1 is established offline with $n_{row} = 43$ and $n_{col} = 7$. As a comparison, both

**Algorithm 2:** Hash table.

**Input:** $\alpha_i$, $F_{zi}$, $(i = f, r)$.
**Output:** $F_{yi}\,(i = f, r)$.
**Step 1:** Compute $n_1$ according to (21).
**Step 2:** Compute the tyre lateral forces $\tilde{M}$ under the tyre load $F_{zi}$ according to (22).
**Step 3:** Compute the keyword $n_2$ according to (23).
**Step 4:** Access the lateral force $F_{yi}$ according to (24).

an uncontrolled front wheel steering vehicle (FWS) and a proportional controller are designed [48,49], where the ratio of the proportional controller is

$$\frac{\delta_f}{\delta_r} = \frac{-b + mav^2/C_f\,(a+b)}{a + mbv^2/C_r\,(a+b)}. \tag{25}$$

The weighting matrices are chosen as $Q = \begin{bmatrix} 500 & 0 \\ 0 & 500 \end{bmatrix}$, $R = \begin{bmatrix} 50 & 0 \\ 0 & 50 \end{bmatrix}$ and $\sigma = 10^6$. The other simulation parameters are shown in Table 2.

The simulation scenario is as follows: the road adhesion coefficient is $\mu = 0.75$, the constraint of the lateral acceleration is $|a_y| \leq 0.75$ g. The constraint of the sideslip angle is $\beta \in [-0.038,\, 0.038]$ rad, which prevents the vehicle from instability [50].

**Remark 3:** In this research, the parameters of controller include the prediction horizon ($T_p$), the weighting matrices ($Q$ and $R$), and the penalty coefficient ($\sigma$), which is usually obtained by trial and error. Compared to the input weighting matric $R$, the large state weighting matric $Q$ quickly drives the state to the ideal values at the expense of large control increment action. Penalizing the term $\|\Delta u(\tau)\|$ with large values of $R$ reduces the control increment action and slows down the rate that the state approaches the ideal values [51].

## 4.1. Cornering maneuver

Here, two tests of the step response with both a low speed and a high speed are carried out.

Table 2. Parameters of simulation.

| Parameter | Value | Parameter | Value |
|---|---|---|---|
| $m$ | 1111 kg | $I_z$ | 2031.4 kg·m$^2$ |
| $a$ | 1.04 m | $b$ | 1.56 m |
| $C_f$ | 39515.0 N/rad | $C_r$ | 39515.0 N/rad |
| $T_p$ | 0.05 s | $\Delta t$ | 0.01 s |
| $\tau_\beta$ | 0.1 | $\tau_\gamma$ | 0.1 |
| $\delta_{fmax}$ | 0.5 rad | $\delta_{rmax}$ | 0.08 rad |

### 4.1.1 Case 1: Low-speed

**Scenario:** The longitudinal speed of the 4WS vehicle is 10 m/s. As shown in Fig. 5, the reference front wheel angle is 0.14 rad. The constraint of yaw rate is $|\gamma| \leq \frac{\mu g}{v} = 0.735$.

Figs. 6-8 are evolutions of the sideslip angle, the yaw rate, and the lateral acceleration of vehicles under three steering modes, respectively. Note that the solid red lines in Figs. 6-8 represent the corresponding constraints. In Figs. 6 and 7, compared with the other schemes, the proposed controller achieves the best tracking performance on the ideal steering characteristic. The sideslip angle of the vehicle under the proportional controller is close to the reference. However, the yaw rate is greater than the related ideal reference, which will result in the so-called oversteer. In addition, the sideslip angle of the uncontrolled

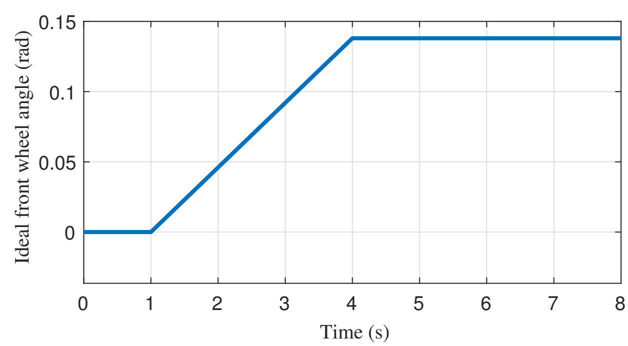


Fig. 5. Reference front wheel angle.

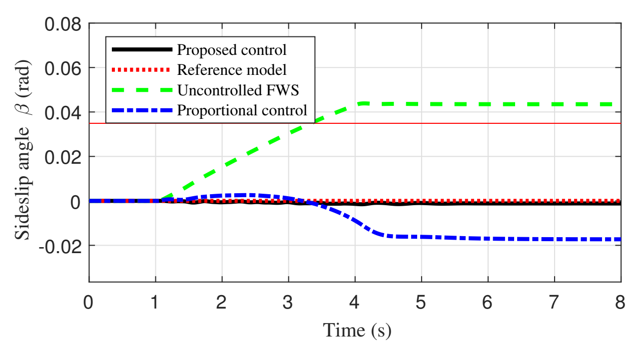


Fig. 6. The evolution of sideslip angle.

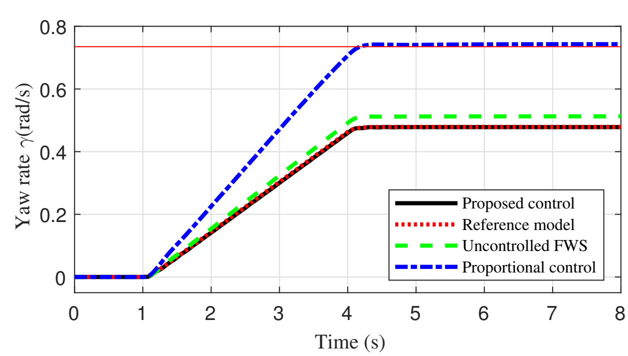


Fig. 7. The evolution of yaw rate.

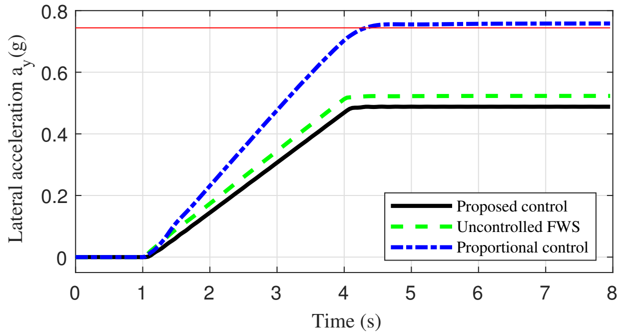


Fig. 8. The evolution of lateral acceleration.

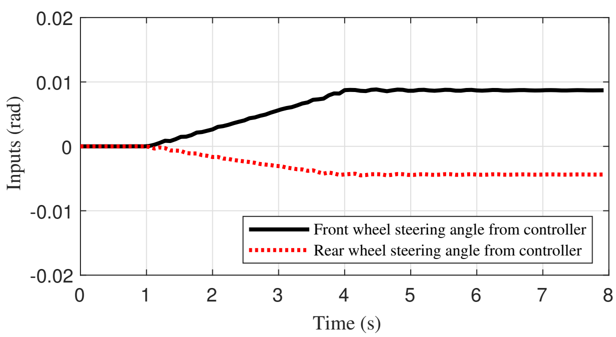


Fig. 9. The evolution of control inputs.

FWS vehicle is much greater than 0.038 rad sometime which might cause the instability problem of vehicles. The evolutions of the 4WS vehicle with the proportional controller shown in Figs. 7 and 8 violate constraints of the yaw rate and the lateral acceleration. Fig. 9 are the control inputs $u = \begin{bmatrix} \delta_f & \delta_r \end{bmatrix}^T$, i.e., the front steering angle and the rear steering angle. The front wheel steering direction and the rear wheel steering direction are opposite, which causes the so-called counter-phase steering mode of four-wheel steering vehicles at a low speed. It can be seen from Fig. 9 that actuators are not saturated.

Simulation results in Case 1 show that the proposed model predictive controller can enhance the handling stability of the 4WS vehicle.

### 4.1.2 Case 2: High-speed

**Scenario:** the steering wheel turns at a fixed angle while the vehicle is traveling in a straight line at a constant speed of 20 m/s. As shown in Fig. 10, the reference front wheel angle is 0.07 rad. The constraint of yaw rate is $|\gamma| \leq \frac{\mu g}{v} = 0.3675$.

The crosswind, which frequently occurs to the vehicle, might seriously affect the handling stability of vehicles. To verify the robustness of the controller, a crosswind experiment is carried out while vehicles are traveling at high speed. The crosswind with the speed of 40 km/h is acted after 2 s.

Figs. 11-13 are evolutions of the sideslip angle, the yaw rate, and the lateral acceleration of vehicles under three steering control modes, respectively. In Figs. 11 and 12, the proposed controller and the proportional controller can improve the handling stability of vehicles with respect to the crosswind disturbance. The sideslip angle of the 4WS vehicle with proposed controller is kept close to zero in the process of the sinusoidal steering, i.e., the attitude of the vehicle is well maintained. Note that the solid red lines in Figs. 11-13 represent the corresponding constraints. The evolutions of the uncontrolled FWS vehicle in Figs. 11 and 13 violates the corresponding constraints. The control inputs, i.e., the front and rear wheel steering angles, are shown in Fig. 14, in which directions of the front and rear wheel steering angles are the same, i.e., the 4WS vehicle

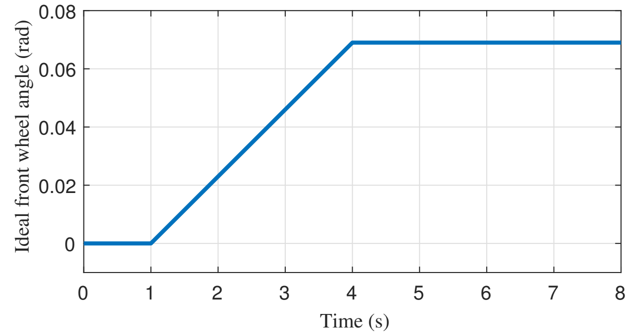


Fig. 10. Reference front wheel angle.

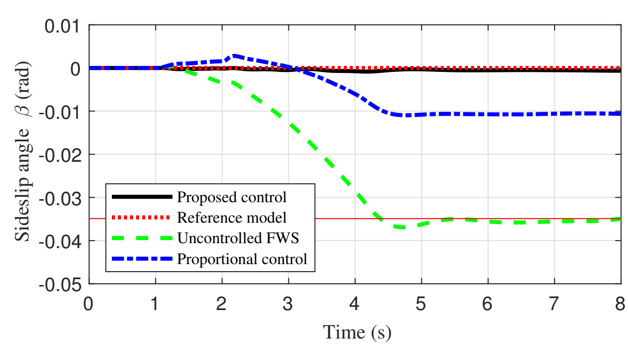


Fig. 11. The evolution of sideslip angle.

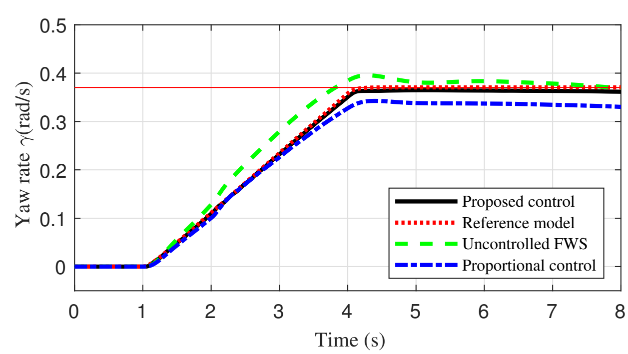


Fig. 12. The evolution of yaw rate.

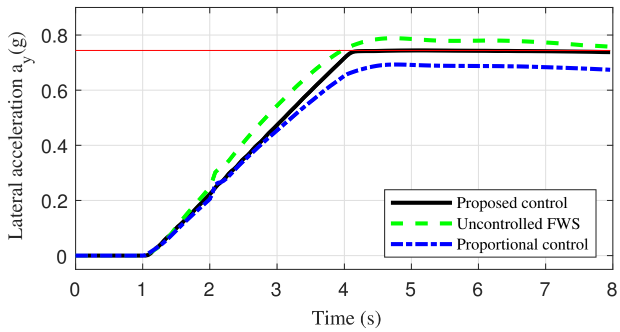


Fig. 13. The evolution of lateral acceleration.

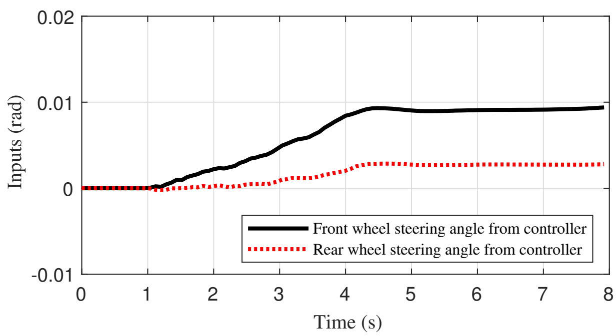


Fig. 14. The evolution of control inputs.

is in-phase steering mode at a high speed. The control inputs are in a reasonable range, and the actuators are not saturated.

Simulation results in Cases 1 and 2 show the effectiveness of the proposed scheme to track accurately the dynamics of the ideal vehicles at different speeds.

## 4.2. Sinusoidal steering angle

Here, the sinusoidal steering test for vehicles with high speed is carried out.

### 4.2.1 Case 3: Sinusoidal steering test

**Scenario:** As shown in Fig. 15, the amplitude and the frequency of the reference front wheel angle are 0.07 rad and 1 rad/s, respectively. The longitudinal speed is 20 m/s. The constraint of yaw rate is $|\gamma| \leq \frac{\mu g}{v} = 0.3675$. The cross-wind is with the speed of 50 km/h.

Figs. 16-18 are evolutions of the sideslip angle, the yaw rate, and the lateral acceleration of vehicles under three steering control modes, respectively. Note that the solid red lines in Figs. 16-18 represent the corresponding constraints. In Figs. 16 and 17, both the sideslip angle and the yaw rate of the vehicle with the proposed controller are very close to that given by the reference model. In Figs. 16-18, the evolutions of vehicles with the proposed controller meet the constraints. However, the front wheel steering vehicle is over-steer, and vehicle with the proportional controller is under-steer. In Fig. 19, the four-wheel

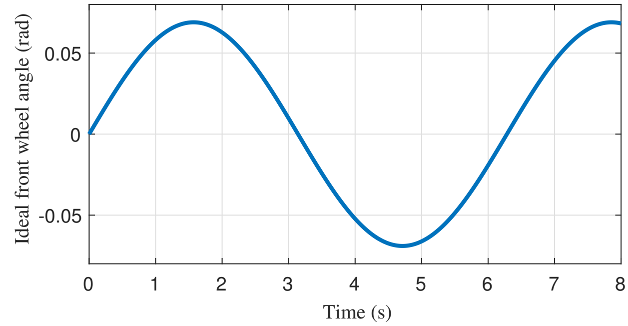


Fig. 15. Reference front wheel angle.

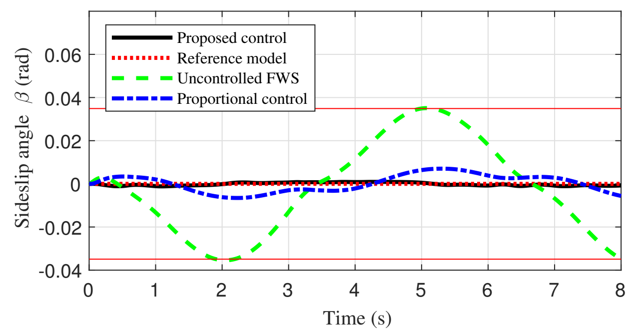


Fig. 16. The evolution of sideslip angle.

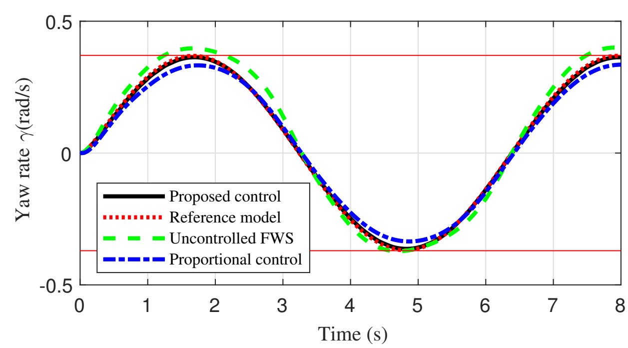


Fig. 17. The evolution of yaw rate.

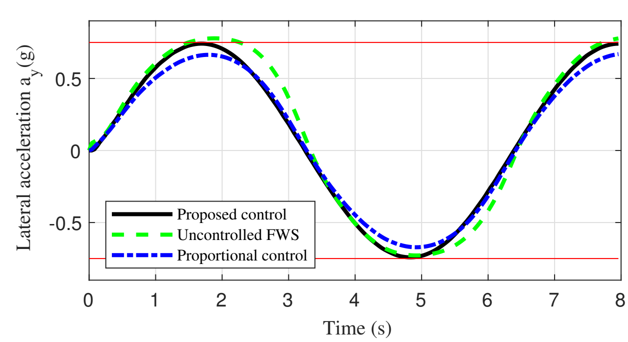


Fig. 18. The evolution of lateral acceleration.

steering vehicle is in-phase steering mode at a high speed. The control inputs are still in a reasonable range, and the actuators are not saturated.

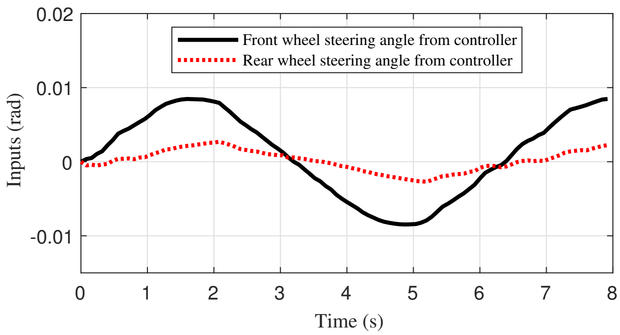


Fig. 19. The evolution of control inputs.

Simulation results of Cases 2 and 3 show the proposed method can improve effectively the handling stability of vehicles at different steering inputs under external disturbances, that is, the controller is robust.

### 4.3. Computational burden

To verify the effectiveness of the map for reducing the computational burden of model predictive controller, the Dugoff tyre model [52] is built as a comparison. The simulation is performed on a desktop computer with 3.6 GHz Intel Core i7-4790 processors.

Fig. 20 is the comparison of computational time. The solid line represents the computational time of model predictive controller with maps, the dash-dot line represents the computational time of model predictive controller with Dugoff tyre model. The average computational time of model predictive controller with maps is 0.00559 s, and the average computational time of the model predictive controller with Dugoff tyre model is 0.00763 s. That is, 26.74% computational burden reduction is achieved with maps. Note that the computational time of the model predictive controller with Dugoff tyre model is greater than the sampling time $\Delta t = 0.01$ s sometimes which causes the vehicle losing control at the next time instant.

Note that in this research, CarSim is used in the simulation, which is a professional software for analyzing vehicle system dynamics with high accuracy. Future research will take the implementation of the proposed controller in real vehicles or small-scale vehicles into account.

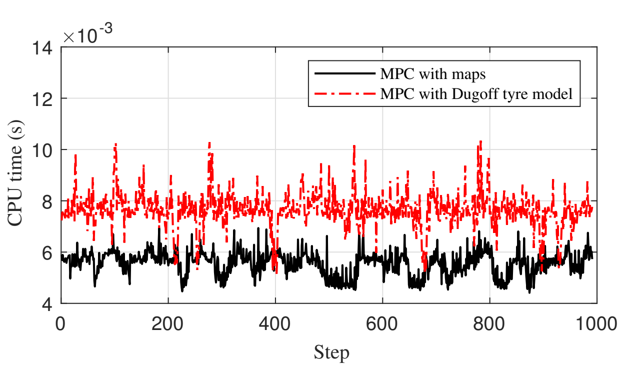


Fig. 20. The comparison of computational time.

## 5. CONCLUSION

In this paper, a nonlinear predictive controller taking the nonlinear characteristics of tyres into account was developed to improve the handling stability of active 4WS vehicles. A model that consists of a nonlinear tyre and a linear dynamic vehicle was presented, in which the nonlinear tyre model was approximated by the map. As a result of introduction of a map, i.e., balance of the computational burden of CPU and the storage burden of ROM, the computational complexity of MPC was exploited. Simulation results in CarSim indicate that the proposed controller could enhance the handling stability of the 4WS vehicle. Furthermore, computational complexity is reduced with the introduction of maps.

The optimization problem based on the hash table is addressed whereas stability of the system with model predictive controller is not discussed. Future works will take into account the effect of the map on the stability of the system.

## CONFLICT OF INTEREST

The authors declare that there is no competing financial interest or personal relationship that could have appeared to influence the work reported in this paper.

## REFERENCES

[1] J. Yoon, W. Cho, B. Koo, and K. Yi, "Unified chassis control for rollover prevention and lateral stability," *IEEE Transactions on Vehicular Technology*, vol. 58, no. 2, pp. 596-609, 2008.

[2] M. Ghaedi, F. Bayat, and A. Fekih. "Robust performance improvement of lateral motion in four-wheel independent-drive electric vehicles," *IEEE Access*, vol. 8, pp. 203146-203157, 2020.

[3] L. Chen, Z. Li, and J. Yang. "Lateral stability control of four-wheel-drive electric vehicle based on coordinated control of torque distribution and ESP differential braking," *Actuators*, vol. 10, no. 6, 135, 2021.

[4] H. E. Russell and J. C. Gerdes, "Design of variable vehicle handling characteristics using four-wheel steer-by-wire," *IEEE Transactions on Control Systems Technology*, vol. 24, no. 5, pp. 1529-1540, 2015.

[5] S. Wagner, T. Weiskircher, D. Ammon, and G. Prokop, "Pivot point-based control for active rear-wheel steering in passenger vehicles," *Vehicle System Dynamics*, vol. 56, no. 8, pp. 1139-1161, 2018.

[6] M. Ataei, A. Khajepour, and S. Jeon, "A novel reconfigurable integrated vehicle stability control with omni actuation systems," *IEEE Transactions on Vehicular Technology*, vol. 67, no. 4, pp. 2945-2957, 2017.

[7] G. D. Yin, N. Chen, J. X. Wang, and J. S. Chen, "Robust control for 4WS vehicles considering a varying tire-road friction coefficient," *International Journal of Automotive Technology*, vol. 11, no. 1, pp. 33-40, 2010.

[8] H. Lv and S. Liu, "Closed-loop handling stability of 4WS vehicle with yaw rate control," *Strojniški Vestnik-Journal of Mechanical Engineering*, vol. 59, no. 10, pp. 595-603, 2013.

[9] B. Li, S. Rakheja, and Y. Feng, "Enhancement of vehicle stability through integration of direct yaw moment and active rear steering," *Proc. of the Institution of Mechanical Engineers, Part D: Journal of Automobile Engineering*, vol. 230, no. 6, pp. 830-840, 2016.

[10] A. Tavasoli, M. Naraghi, and H. Shakeri, "Optimized coordination of brakes and active steering for a 4WS passenger car," *ISA transactions*, vol. 51, no. 5, pp. 573-583, 2012.

[11] X. Wu, M. Zhang, and M. Xu, "Active tracking control for steer-by-wire system with disturbance observer," *IEEE Transactions on Vehicular Technology*, vol. 68, no. 6, pp. 5483-5493, 2019.

[12] Z. Sun, J. Zheng, Z. Man, M. Fu, and R. Lu, "Nested adaptive super-twisting sliding mode control design for a vehicle steer-by-wire system," *Mechanical Systems and Signal Processing*, vol. 122, pp. 658-672, 2019.

[13] H. Zhao, B. Wang, G. Zhang, and Y. Feng, "Energy saving design and control of steering wheel system of steering by wire vehicle," *IEEE Access*, vol. 7, pp. 44307-44316, 2019.

[14] L. Tan, S. Yu, Y. Guo, and H. Chen, "Sliding-mode control of four wheel steering systems," *Proc. of IEEE International Conference on Mechatronics and Automation*, pp. 1250-1255, 2017.

[15] M. Canale and L. Fagiano, "Stability control of 4WS vehicles using robust imc techniques," *Vehicle System Dynamics*, vol. 46, no. 11, pp. 991-1011, 2008.

[16] C. Liu, W. Sun, and J. Zhang, "Adaptive sliding mode control for four-wheel SBW system with ackerman geometry," *ISA transactions*, vol. 96, pp. 103-115, 2020.

[17] S. Yu, J. Wang, Y. Wang, and H. Chen, "Disturbance observer based control for four wheel steering vehicles with model reference," *IEEE/CAA Journal of Automatica Sinica*, vol. 5, no. 6, pp. 1121-1127, 2016.

[18] J. Wang, S. Yu, and H. Chen, "Model following control of active 4WS vehicle based on constrained output feedback $H_\infty$ control," *Information and Control* (in Chinese), vol. 45, no. 1, pp. 53-59, 2016.

[19] F. X. Xu, X. H. Liu, W. Chen, C. Zhou, and B. W. Cao, "Improving handling stability performance of four-wheel steering vehicle based on the $H_2/H_\infty$ robust control," *Applied Sciences*, vol. 9, no. 5, pp. 857, 2019.

[20] S. Yu, J. Wang, J. S. Kim, H. Chen, and F. Allgöwer, "Quasi full information feedback control law of linear systems," *IFAC-PapersOnLine*, vol. 50, no. 1, pp. 904-909, 2017.

[21] S. Yu, L. Tan, W. Wang, and H. Chen, "Control of active four wheel steering vehicle based on triple-step method," *Journal of Jilin University (Engineering and Technology Edition)*, vol. 49, no. 3, pp. 934-942, 2019.

[22] J. Wurts, J. L. Stein, and T. Ersal, "Collision imminent steering at high speed using nonlinear model predictive control," *IEEE Transactions on Vehicular Technology*, vol. 69, no. 8, pp. 8278-8289, 2020.

[23] M. Fnadi, F. Plumet, and F. Benamar, "Model predictive control based dynamic path tracking of a four-wheel steering mobile robot," *Proc. of International Conference on Intelligent Robots and Systems*, IEEE, pp. 4518-4523, 2019.

[24] S. Horiuchi, K. Okada, and S. Nohtomi, "Effects of integrated control of active four wheel steering and individual wheel torque on vehicle handling and stability-a comparison of alternative control strategies," *The Dynamics of Vehicles on Roads and on Tracks*, CRC Press, pp. 680-691, 2021.

[25] X. Liu, W. Wang, X. Li, F. Liu, Z. He, Y. Yao, H. Ruan, and T. Zhang, "MPC-based high-speed trajectory tracking for 4wis robot," *ISA Transactions*, vol. 123, pp. 413-424, 2022.

[26] P. Hang, F. Luo, S. Fang, and X. Chen, "Path tracking control of a four-wheel-independent-steering electric vehicle based on model predictive control," *Proc. of 36th Chinese Control Conference (CCC)*, IEEE, pp. 9360-9366, 2017.

[27] K. Shi, X. Yuan, and Q. He, "Double-layer dynamic decoupling control system for the yaw stability of four wheel steering vehicle," *International Journal of Control, Automation, and Systems*, vol. 17, no. 5, pp. 1255-1263, 2019.

[28] R. Wang, G. Yin, and X. Jin, "Robust adaptive sliding mode control for nonlinear four-wheel steering autonomous vehicles path tracking systems," *Proc. of IEEE 8th International Power Electronics and Motion Control Conference (IPEMC-ECCE Asia)*, IEEE, pp. 2999-3006, 2016.

[29] Q. J. Liu and S. Z. Chen, "The control of the braking stability of active rear wheel steering vehicle based on LQR," *Applied Mechanics and Materials*, vol. 416, pp. 909-913, 2013.

[30] S. Yu, W. Li, W. Wang, and T. Qu, "Nonlinear control of active four wheel steer-by-wire vehicles," *IEEE Access*, vol. 7, pp. 127117-127127, 2019.

[31] R. Liu, M. Wei, N. Sang, and J. Wei, "Research on curved path tracking control for four-wheel steering vehicle considering road adhesion coefficient," *Mathematical Problems in Engineering*, vol. 2020, Article ID 3108589, 2020.

[32] H. Zheng, S. Yang, and B. Li, "Optimization control for 4WIS electric vehicle based on the coincidence degree of wheel steering centers," *SAE International Journal of Vehicle Dynamics, Stability, and NVH*, vol. 2, no. 3, pp. 169-184, 2018.

[33] K. Guo, D. Lu, S. K. Chen, W. C. Lin, and X. P. Lu, "The unitire model: A nonlinear and non-steady-state tyre model for vehicle dynamics simulation," *Vehicle System Dynamics*, vol. 43, no. sup1, pp. 341-358, 2005.

[34] M. Kissai, B. Monsuez, A. Tapus, and D. Martinez, "A new linear tire model with varying parameters," *Proc. of 2nd IEEE International Conference on Intelligent Transportation Engineering (ICITE)*, IEEE, pp. 108-115, 2017.

[35] Q. Wang, Y. Zhao, Y. Deng, H. Xu, H. Deng, and F. Lin, "Optimal coordinated control of ARS and DYC for four-wheel steer and in-wheel motor driven electric vehicle with unknown tire model," *IEEE Transactions on Vehicular Technology*, vol. 69, no. 10, pp. 10809-10819, 2020.

[36] C. Chen and Y. Jia, "Nonlinear decoupling control of four-wheel-steering vehicles with an observer," *International Journal of control, Automation and systems*, vol. 10, no. 4, pp. 697-702, 2012.

[37] M. Nagai, Y. Hirano, and S. Yamanaka, "Integrated robust control of active rear wheel steering and direct yaw moment control," *Vehicle System Dynamics*, vol. 29, no. S1, pp. 416-421, 1998.

[38] Q. Meng, Z.-Y Sun, and Y. Li, "Finite-time controller design for four-wheel-steering of electric vehicle driven by four in-wheel motors," *International Journal of Control, Automation, and Systems*, vol. 16, no. 4, pp. 1814-1823, 2018.

[39] M. Nagai, M. Shino, and F. Gao, "Study on integrated control of active front steer angle and direct yaw moment," *JSAE review*, vol. 23, no. 2, pp. 309-315, 2002.

[40] J. Zhang, H. Zheng, and M. Zhao, "Analysis of vehicle steering stability of nonlinear four wheel steering based on sliding mode control," SAE Technical Paper 2018-01-1593, 2018.

[41] L. Li, G. Jia, J. Chen, H. Zhu, D. Cao, and J. Song, "A novel vehicle dynamics stability control algorithm based on the hierarchical strategy with constrain of nonlinear tyre forces," *Vehicle System Dynamics*, vol. 53, no. 8, pp. 1093-1116, 2015.

[42] X. Yang, Z. Wang, and W. Peng. "Coordinated control of AFS and DYC for vehicle handling and stability based on optimal guaranteed cost theory," *Vehicle System Dynamics*, vol. 47, no. 1, pp. 57-79, 2009.

[43] J. He, D. A. Crolla, M. C. Levesley, and W. J. Manning, "Integrated active steering and variable torque distribution control for improving vehicle handling and stability,"SAE Technical Paper 2004-01-1071, 2004.

[44] C. Y. Chen and F. Ye, "Particle swarm optimization algorithm and its application to clustering analysis," *Proc. of 17th Conference on Electrical Power Distribution*, IEEE, pp. 789-794, 2012.

[45] F. Bayat, T. A. Johansen, and A. A. Jalali, "Using hash tables to manage the time-storage complexity in a point location problem: Application to explicit model predictive control," *Automatica*, vol. 47, no. 3, pp. 571-577, 2011.

[46] T. A. Johansen, F. Jackson, and R. Schreiber, "Hardware synthesis of explicit model predictive controllers," *IEEE Transactions on Control Systems Technology*, vol. 15, no. 1, pp. 191-197, 2006.

[47] A. Molina, K. Rajamani, and K. Azadet, "Digital predistortion using lookup tables with linear interpolation and extrapolation: Direct least squares coefficient adaptation," *IEEE Transactions on Microwave Theory and Techniques*, vol. 65, no. 3, pp. 980-987, 2016.

[48] Y. Xia, M. Lin, J. Zhang, M. Fu, C. Li, S. Li, and Y. Yang, "Trajectory planning and tracking for four-wheel steering vehicle based on differential flatness and active disturbance rejection controller," *International Journal of Adaptive Control and Signal Processing*, vol. 35, no. 11, pp. 2214-2244, 2021.

[49] Z. Jiang and B. Xiao, "LQR optimal control research for four-wheel steering forklift based-on state feedback," *Journal of Mechanical Science and Technology*, vol. 32, no. 6, pp. 2789-2801, 2018.

[50] A. T. Van Zanten, "Bosch ESP systems: 5 years of experience," SAE Technical Paper 2000-01-1633, 2000.

[51] J. Rawlings and D. Mayne, "Postface to model predictive control: Theory and design," *Nob Hill Pub*, vol. 5, pp. 155-158, 2012.

[52] H. Mirzaeinejad, M. Mirzaei, and S. Rafatnia, "A novel technique for optimal integration of active steering and differential braking with estimation to improve vehicle directional stability," *ISA Transactions*, vol. 80, pp. 513-527, 2018.

**Shuyou Yu** received his B.S. and M.S. degrees in control science and engineering from Jilin University, China, in 1997 and 2005, respectively, and a Ph.D. degree in engineering cybernetics from the University of Stuttgart, Germany, in 2011. From 2010 to 2011, he was a Research and Teaching Assistant with the Institute for Systems Theory and Automatic Control, University of Stuttgart. In 2012, he joined the Department of Control Science and Engineering, Jilin University, as a Faculty Member, where he is currently a Full Professor. His main research interests include model predictive control, robust control, and its applications in mechatronic systems.

**Wenbo Li** received his B.S. degree in automation from Jilin University, Changchun, China, in 2019, where he is currently pursuing a Ph.D. degree in control science and engineering, with a focus on the vehicle stability control.

**Yongfu Li** received his Ph.D. degree in control science and engineering from Chongqing University, Chongqing, China, in 2012. He is currently a full professor of control science and engineering and the founding Director of Key Laboratory of Intelligent Air-Ground Cooperative Control (IACC) for Universities in Chongqing as well as the founding Director of International Research Center for Intelligent Connected Vehicles and Transportation (ICVT) in Chongqing at Chongqing University of Posts and Telecommunications. His research interests include automated driving, connected and automated vehicles, and intelligent transportation systems.

**Hong Chen** received her B.S. and M.S. degrees in process control from Zhejiang University, China, in 1983 and 1986, respectively, and a Ph.D. degree in system dynamics and control engineering from the University of Stuttgart, Germany, in 1997. In 1986, she joined the Jilin University of Technology, China. From 1993 to 1997, she was a Wissenschaftlicher Mitarbeiter with the Institut für Systemdynamik und Regelungstechnik, University of Stuttgart. Since 1999, she has been a Professor at Jilin University and hereafter a Tang Aoqing Professor. From 2015 to 2019, she served as the Director of the State Key Laboratory of Automotive Simulation and Control. In 2019, she joined Tongji University as a Distinguished Professor. Her current research interests include model predictive control, nonlinear control, and applications in mechatronic systems focusing on automotive systems.

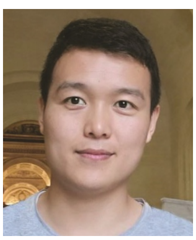

**Hongqing Chu** received his B.S. degree in vehicle engineering from Shandong University of Technology, China, in 2012, and a Ph.D. degree in control theory and control engineering from Jilin University, China, in 2017. He is currently an assistant professor at Tongji University, China. His current research interests include advanced driver-assistance systems, nonlinear control of DC motor drive, and vehicle powertrain control.

**Baojun Lin** received his B.E. degree in electrical technology from Harbin University of Science and Technology in 1997, an M.S. degree in signal and information processing from Jilin University in 2005, and a Ph.D. degree in material processing engineering from Jilin University in 2009. He is currently an Associate Professor at Jilin University. His research interests include CNC system, programmable logic controller, motor speed regulation, and its applications in mechatronic systems.

**Jianhua Yu** received his B.E. degree from the Tsinghua University, China, in 1989, and an M.S. degree in the internal combustion engine from Beijing Institute of Technology, China, in 1997. He is currently working at Dongfeng Commercial Vehicle Co., Ltd.